# Journal Pre-proof

Effective inhibition of breast cancer stem cell properties by quercetin-loaded solid lipid nanoparticles via reduction of Smad2/Smad3 phosphorylation and  $\beta$ -catenin signaling pathway in triple-negative breast cancer

Mahdi Hatami, Maryam Kouchak, Alireza Kheirollah, Layasadat Khorsandi, Mojtaba Rashidi

PII: S0006-291X(23)00377-7

DOI: https://doi.org/10.1016/j.bbrc.2023.03.077

Reference: YBBRC 48496

To appear in: Biochemical and Biophysical Research Communications

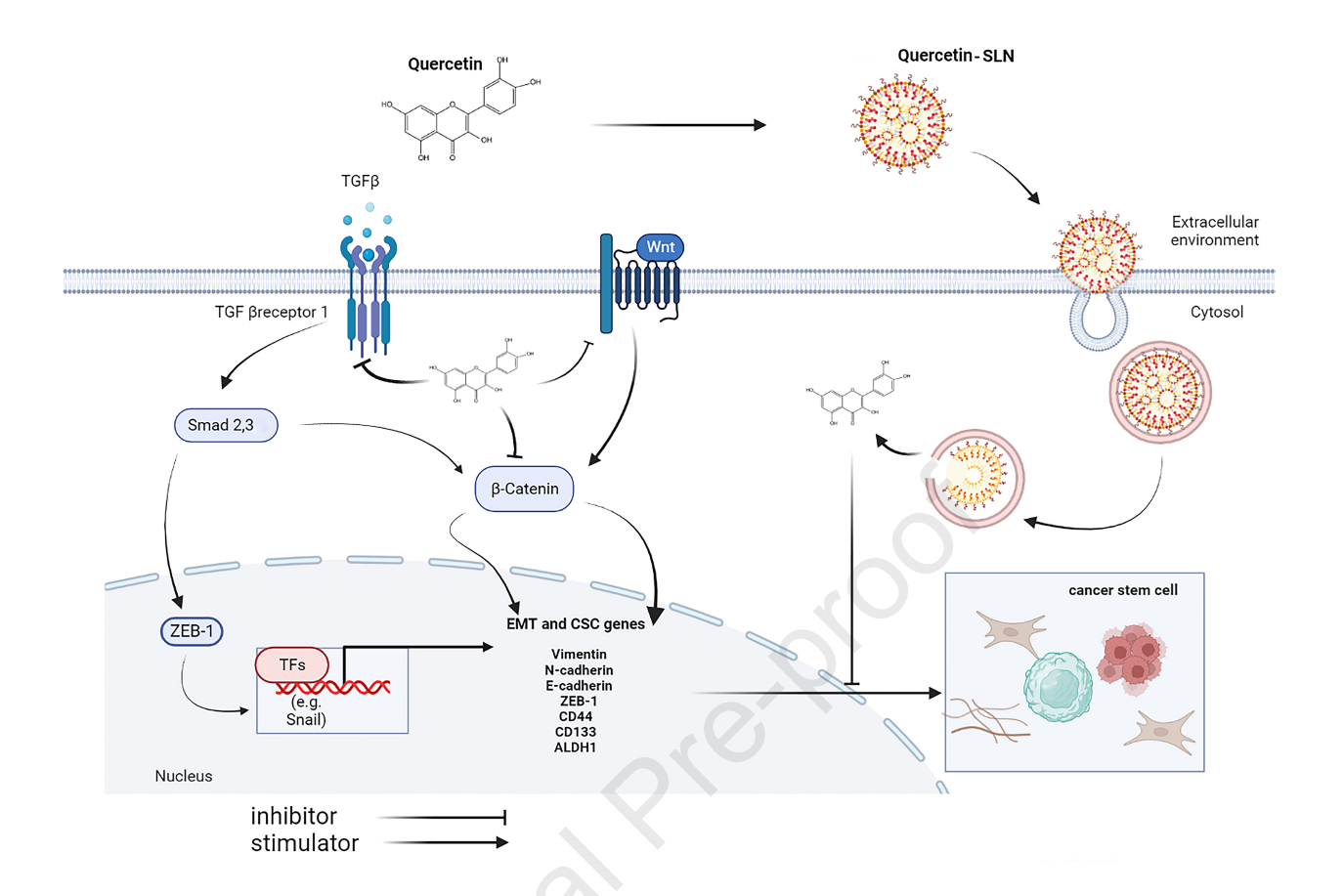
Received Date: 5 March 2023
Revised Date: 25 March 2023
Accepted Date: 30 March 2023

Please cite this article as: M. Hatami, M. Kouchak, A. Kheirollah, L. Khorsandi, M. Rashidi, Effective inhibition of breast cancer stem cell properties by quercetin-loaded solid lipid nanoparticles via reduction of Smad2/Smad3 phosphorylation and  $\beta$ -catenin signaling pathway in triple-negative breast cancer, *Biochemical and Biophysical Research Communications* (2023), doi: https://doi.org/10.1016/j.bbrc.2023.03.077.

This is a PDF file of an article that has undergone enhancements after acceptance, such as the addition of a cover page and metadata, and formatting for readability, but it is not yet the definitive version of record. This version will undergo additional copyediting, typesetting and review before it is published in its final form, but we are providing this version to give early visibility of the article. Please note that, during the production process, errors may be discovered which could affect the content, and all legal disclaimers that apply to the journal pertain.

© 2023 Published by Elsevier Inc.





# Effective Inhibition of Breast Cancer Stem Cell Properties by Quercetin-Loaded Solid Lipid Nanoparticles via Reduction of Smad2/Smad3 Phosphorylation and β-Catenin Signaling Pathway in Triple-Negative Breast Cancer

Mahdi Hatami<sup>1,2</sup>, Maryam Kouchak<sup>3,4</sup>, Alireza Kheirollah<sup>2</sup>, Layasadat Khorsandi<sup>1</sup>, Mojtaba Rashidi<sup>1,2\*</sup>

<sup>1</sup>Cellular and Molecular Research Center, Medical Basic Sciences Research Institution, Ahvaz Jundishapur University of Medical Sciences, Ahvaz, Iran.

Fax: +98 61 33738632, Mobile:09166131031

#### Abstract

Background: The presence of cancer stem cells (CSCs) is a major cause of resistance to cancer therapy and recurrence. Triple-negative breast cancer (TNBC) is a subtype that responds poorly to therapy, making it a significant global health issue. Quercetin (QC) has been shown to affect CSC viability, but its low bioavailability limits its clinical use. This study aims to increase the effectiveness of QC in inhibiting CSC generation by using solid lipid nanoparticles (SLNs) in MDA-MB231 cells.

Materials and Methods: After treating MCF-7 and MDA-MB231 cells with 18.9  $\mu$ M and 13.4  $\mu$ M of QC and QC-SLN for 48 hours, respectively, cell viability, migration, sphere formation, protein expression of  $\beta$ -catenin, p-Smad 2 and 3, and gene expression of EMT and CSC markers were evaluated.

Results: The QC-SLN with particle size of 154 nm, zeta potential of -27.7 mV, and encapsulation efficacy of 99.6% was found to be the most effective. Compared to QC, QC-SLN significantly reduced cell viability, migration, sphere formation, protein expression of  $\beta$ -catenin and p-Smad 2 and 3, and gene expression of CD<sub>44</sub>, zinc finger E-box binding homeobox 1 (ZEB1), vimentin, while increasing the gene expression of E-cadherin.

Conclusions: Our findings demonstrate that SLNs improve the cytotoxic effect of QC in MDA-MB231 cells by increasing its bioavailability and inhibiting epithelial-mesenchymal transition (EMT), thereby effectively inhibiting CSC generation. Therefore, SLNs could be a promising new treatment for TNBC, but more in vivo studies are needed to confirm their efficacy.

Keywords: Solid lipid nanoparticles (SLN), Quercetin, Invasive, Epithelial-mesenchymal transition (EMT), Cancer stem cell (CSC)

<sup>&</sup>lt;sup>2</sup> Department of Clinical Biochemistry, Faculty of Medicine, Ahvaz Jundishapur University of Medical Sciences, Ahvaz, Iran

<sup>&</sup>lt;sup>3</sup> Nanotechnology Research Center, Ahvaz Jundishapur University of Medical Sciences, Ahvaz, Iran

<sup>&</sup>lt;sup>4</sup> Department of Pharmaceutics, Faculty of Pharmacy, Ahvaz Jundishapur University of Medical Sciences, Ahvaz, Iran

<sup>\*</sup> Correspondence: ms\_rashidi60@yahoo.com, rashidi-mo@ajums.ac.ir Tel: +98 61 33738632;

#### 1.Introduction

Breast cancer is a significant cause of cancer-related mortality among women globally [1]. Triplenegative breast cancer (TNBC), a subtype of breast cancer, is characterized by a poor prognosis and a low response to chemotherapy, often resulting in recurrence and metastasis [2,3]. Treatment failure in cancer is primarily due to the presence of cancer stem cells (CSCs) [4].

The CSC theory posits that a small population of stem-like cells with self-renewal and differentiation abilities are resistant to conventional cancer therapies, such as chemotherapy and radiation. This resistance can lead to tumor relapse, aggressiveness, and carcinogenesis [5]. Hence, targeting CSCs is crucial in cancer treatment. Numerous studies have demonstrated that CSCs play a pivotal role in the ability of tumors to metastasize and acquire resistance to chemotherapy. They have been identified in various solid tumors, including breast tumors and other cancers [6]. The EMT process is considered the most crucial step in CSC generation.

The epithelial-to-mesenchymal transition (EMT) plays a crucial role in cancer progression and development [7]. During EMT, the loss of E-cadherin triggers a cascade of signal transduction pathways and increases mesenchymal markers such as vimentin and N-cadherin [8]. Therefore, these pathways are important targets for drugs that inhibit EMT and prevent the formation of CSCs [9,10]. Specifically, the Wnt/β-catenin and TGFβ-R1/Smad2/3 signaling pathways activate EMT and maintain CSC characteristics. Previous research has demonstrated that the Wnt/β-catenin signaling pathway is involved in targeted gene transcription in many types of cancer [11]. In breast cancer patients, oncogenes have been found to trigger dysfunction of the Wnt/β-catenin pathway, and breast CSCs have been shown to rely on this pathway [12].

Breast cancer is typically treated with surgery, radiotherapy, and chemotherapy, all of which may cause significant side effects. However, in the recent years, natural-based remedies have emerged as a potential alternative treatment option.

Quercetin (QC) is a natural component that has been found to possess anti-inflammatory and anti-cancer properties. It is commonly present in many fruits and vegetables, such as apples, red onions, and radish leaves [13-16]. Studies have shown that QC can inhibit EMT and prevent the generation of CSCs .However, the clinical application of QC is limited due to its low bioavailability [17,18]. To address this issue, recent research has explored various approaches to improving the bioavailability of QC, one of which involves using solid lipid nanoparticles (SLNs) as a carriers. SLNs are composed of lipids and are capable of effectively encapsulating drugs, including both chemical and natural drugs such as tamoxifen and pomegranate extract. This lipid structure helps protect the drug from chemical breakdown, increasing its half-life and leading to a slow release and enhanced effectiveness of drug therapy [19-23].

The objective of this study was to investigate the impact of using QC-SLN compared to QC on two crucial factors involved in the progression of EMT, namely  $\beta$ -catenin and Smad 2/3. In addition, the study aimed to assess the inhibitory effect of EMT using both sphere formation and wound healing assays. Despite numerous investigations into the anti-tumor effects of nature-derived materials loaded with SLN, little attention has been given to their molecular mechanisms of action on EMTs and CSCs [21,24].

#### 2. Materials and methods

# 2.1. Preparation of QC-SLN

To prepare the QC-SLNs, a mixture of 4.75 g of Compritol 888 ATO (Glyceryl, Dibehenate, Gattefossé, France) and 100 mg of QC was thoroughly mixed at a temperature of 75°C. Separately, 0.25 g of oleic acid and 0.5 g of lecithin were added to deionized water and heated to 80°C, then stirred for 5 minutes. The resulting solution was sonicated with the initial mixture using an Elmasonic S60H sonicator (Global Industrial, USA). To create a nanoemulsion, 4 mL of 1% polyvinyl alcohol (PVA) solution was added to the mixture at 3°C, followed by homogenization at 10,000 rpm using a Heidolph homogenizer (Heidolph Schüttler, Germany). The resulting suspension underwent two rounds of centrifugation at 5°C and 25,000 RCF for a total of 20 minutes. The QC-SLNs were then stored in sealed and refrigerated containers until needed.

### 2.2. Fourier Transform Infrared (FTIR)

After producing the QC-SLNs, their interaction was confirmed by analyzing their FTIR spectra using a (VERTEX 70v, Bruker, USA) spectrometer. The collected spectra were utilized to validate the chemical interaction between QC and SLNs. Pellets were formed by crushing the samples at a force of 200 kg/cm<sup>2</sup> using KBr. The FTIR spectra of QC, QC-SLN, and blank-SLN were recorded within the range of 400-4000 cm<sup>-1</sup> with a resolution of 1 cm<sup>-1</sup>.

# 2.3. Transmission Electron Microscopy (TEM)

The morphology of the QC-SLNs was analyzed using a transmission electron microscope (ZEISS LEO 906 E, Germany). To prepare the samples, a drop of the SLN was deposited onto a carbon-coated copper grid to create a thin liquid coating. The samples were then collected on filter paper and air-dried for 5 minutes at room temperature. The resulting dried samples were then examined using the transmission electron microscope to observe the shape and size of the SLNs.

#### 2.4. Particle Size and Zeta Potential

The average particle size, zeta potential, and polydispersity index (PDI) of the QC-SLNs were determined using a nanosizer and zetasizer (Malvern, England).

### 2.5. Encapsulation Efficiency

The QC-SLN suspension was subjected to a total of 25 minutes of centrifugation at 25,000 rpm, and the amount of QC present in the supernatant was determined at a wavelength of 256 nm using a spectrophotometer (Ultrospec 3000, Pharmacia Biotech, USA). The encapsulation efficiency (EE) was calculated using the following formula [25,26]. EE (%) =100 (Di - Df) /Di

In this equation, Di represents the initial drug, and Df indicates the remaining drug concentration in the supernatant. The drug loading (DL) was calculated by first dissolving QC-SLN in methanol and then measuring the amount of QC present in the solution using a spectrophotometer set to 256 nm. To determine the DL%, we utilized the following formula: DL (%) = 100 (loaded drug/weight of lipid).

# 2.6. In vitro drug release

The quantity of QC released from QC-SLNs was determined using the dialysis bag method with a molecular weight cut-off of 12,000 Da (Sigma-Aldrich, USA) as the receptor phase and a phosphate buffer solution (pH 7.4) at 37°C. Samples were collected at regular intervals and analyzed using spectrophotometry at 256 nm [27].

#### 2.7. Cell Culture

MCF-7 and MDA-MB231 breast cancer cell lines, as well as normal lung fibroblast cells MRC5, were cultured in DMEM high glucose medium supplemented with streptomycin (100 U/mL), fetal bovine serum (FBS) (10%), and penicillin (100 mg/mL), which were purchased from the Iranian Pasteur Research Center. The cells were maintained at 37 °C, 95% humidity, and 5% CO2. After 24 and 48 hours of incubation, various concentrations of QC (ranging from 0 to 400  $\mu$ M), QC-SLN, and blank SLN (ranging from 2.5 to 50  $\mu$ M) were used to determine the IC50 value.

# 2.8. Cell Viability

The three cell lines were seeded at  $4 \times 10^3$  cells per well in 96-well plates to determine cell viability under treatment. Following treatment with QC, QC-SLN, and Blank-SLN for 24 and 48 hours, 0.5 mg/mL MTT solution was added to each well and incubated for four hours at 37°C in the dark. After draining the wells,  $100 \,\mu\text{L}$  of DMSO was added, and absorbance was measured at 570 nm using an ELISA reader (BioTek, ELx800, USA).[28].

# 2.9. Real-Time Polymerase Chain Reaction

The experimental procedure for gene expression analysis involved several steps. First, total RNA was isolated from  $10^6$  cells using RNX-Plus Solution, and the purity and integrity of the RNA were evaluated using the A260/A280 ratio and agarose gel electrophoresis. Next, cDNA was synthesized from the RNA using a 20  $\mu$ l reaction mixture according to the manufacturer's instructions. The primers used for gene expression quantification were listed in Supplementary Table S1, and PCR amplification was carried out for 40 cycles for 10 minutes at 96° C, 15 seconds at 95°C, 30 seconds at 60°C, and 34 seconds at 60°C. Finally, GAPDH was used as a housekeeping gene to normalize the expression levels, and the fold changes in gene expression were calculated using the  $2^{-\Delta\Delta CT}$  formula.

#### 2.10. Sphere Formation Assay

The sphere formation assay is a commonly employed method for culturing stem cells [29]. In this study, we utilized this technique to assess the impact of treatments on the inhibition of CSCs. Specifically, we cultured breast cancer cells in a specialized 6-well ultra-low attachment plate (Corning Inc., Corning, NY) at a density of 100,000 cells per well, in DMEM medium supplemented with 20 ng/mL of epidermal growth factor (EGF) and 20 ng/mL of basic fibroblast growth factor (FGF) from Invitrogen Inc., as well as 1% streptomycin and penicillin. The cells were incubated at 37°C, in a humidified atmosphere of 95% air and 5% CO2, for a period of 7 days. Subsequently, to evaluate the effect of treatments on CSC growth, the culture was supplemented with QC and QC-SLN for 48 hours. Finally, using Image J software, spheres with a diameter greater than 50 µm were quantified.

#### 2.11. Cell Migration Assay

The wound-healing test was used to evaluate the impact of QC and QC-SLN on cell migration at 24 and 48 hours. In brief, MCF-7 and MDA-MB 231 cells were seeded in 6-well plates and allowed to reach greater than 90% confluency. A 5  $\mu$ L pipet tip was then used to create a "wound" in the cell layer. After washing the cells with PBS to remove cell debris and non-attached cells, the cells were treated with 18.9  $\mu$ M and 13.4  $\mu$ M of QC and QC-SLN, respectively. Images were taken at 0, 24, and 48 hours of incubation with QC and QC-SLN. The distance of cell migration was calculated using the National Institutes of Health in Bethesda, United States (NIH) Image J software, using the formula: The rate of migration = [(T0 – Th)/T0] × 100.

#### 2.12. Western blot Analysis

After treating breast cancer cells, they were washed with PBS with a pH of 7.4 and then harvested in a RIPA (radioimmunoprecipitation) lysis solution containing protease inhibitors. The proteins were then separated using the SDS-PAGE technique. Both the primary and secondary antibodies, including anti-p-Smad 2, 3, and anti- $\beta$ -catenin antibodies, were supplied by Santa Cruz Biotechnology. Specific proteins were located and visualized using a detection ECL kit manufactured by Abcam in the United States. The band density was calculated using the NIH Image J software.

### 2.13. Statistical Analysis

The data were presented as mean  $\pm$  SD and were obtained from three independent experiments. Statistical analysis was performed using GraphPad Prism 8 software (GraphPad Software V8, San Diego, CA). One-way analysis of variance (ANOVA) followed by the least significant difference (LSD) post hoc test was used to compare the groups, and p < 0.05 was considered statistically significant.

#### 3. Results

#### 3.1. Characterization of QC-SLNs

The investigated nanoparticles had a negative zeta potential of approximately -27.7 mV, which prevented aggregation and ensured long-term stability. The polydispersity index (PDI) value of

QC-SLN was  $0.50 \pm 0.04$ , indicating a uniform distribution of nanoparticles throughout the sample. Transmission electron microscopy (TEM) images showed spherical nanoparticles with smooth surfaces (Figure 1). The average nanoparticle size was  $154 \pm 22.5$  nm, which was consistent with the dynamic light scattering (DLS) measurement of 156 nm. Notably, the average particle size was smaller than the expected range of 156 nm.

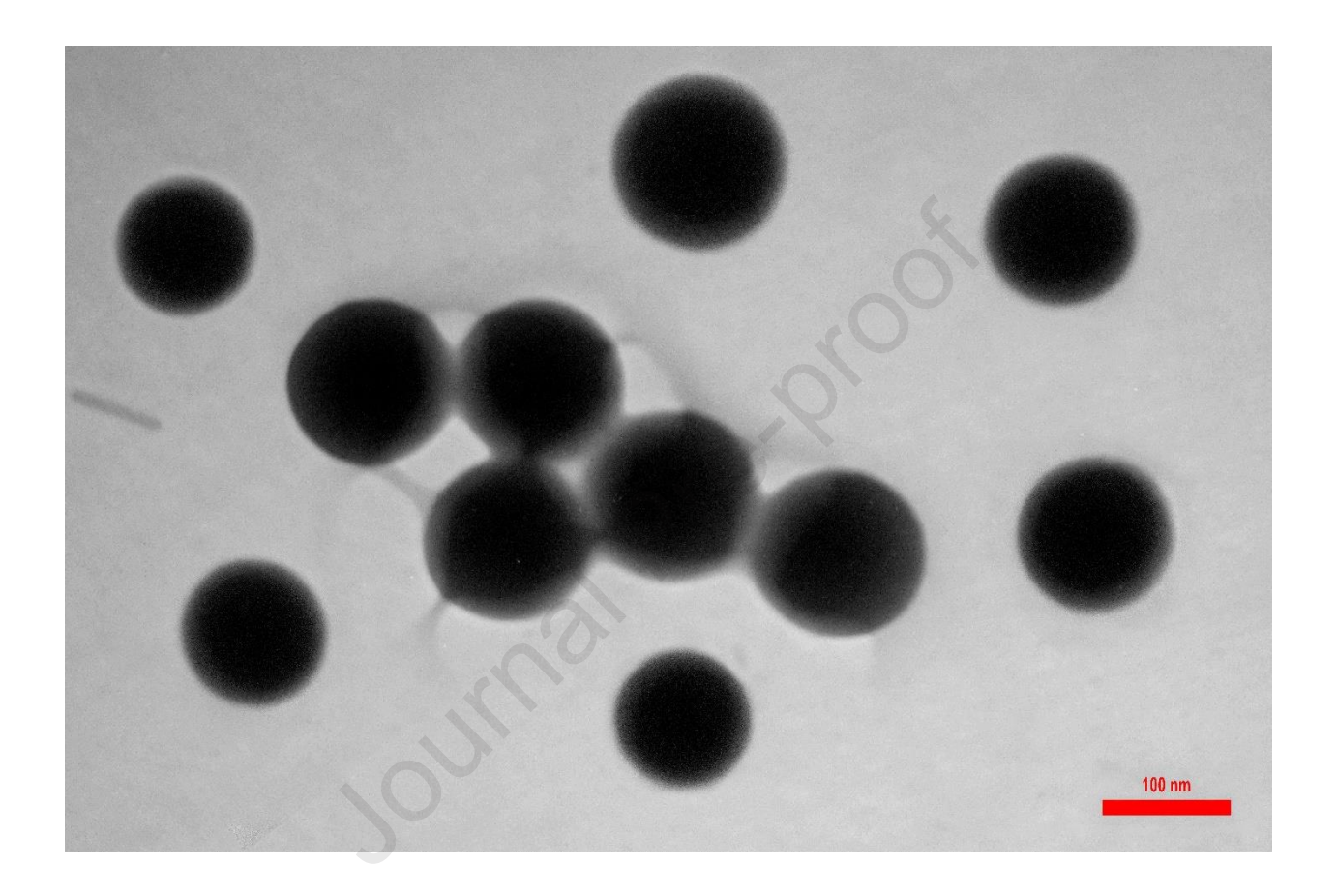


Figure 1. A micrograph produced by the TEM of QC-SLN. Scale bar: 100 nm.

### 3.2. Drug Release Profile

Supplementary Figure S2 shows distinct release characteristics of the QC solution, while QC-SLN exhibited sustained release over three days, with 65% of the drug released in the first 12 hours and a gradual increase to 90% over the remaining time.

# 3.3. FTIR Analysis

Supplementary Figure S3 presents the FTIR test results, revealing characteristic peaks of quercetin at O-H stretching (3850–3200 cm-1), C=O stretching (1635 cm-1), C-C stretching (1659 cm-1), C-H bending (1463, 1379 cm-1), C-O stretching in the ring structure (1262 cm-1), and C-O stretching in the ring structure (1109 -1056 cm-1). Notably, no deletions were observed in the functional group peaks of QC-SLN, thus confirming the appropriate structure of QC in conjunction with other substances utilized during QC-SLN production. These findings align with those reported in a previous study [30].

# 3.4. Cell Viability and Proliferation

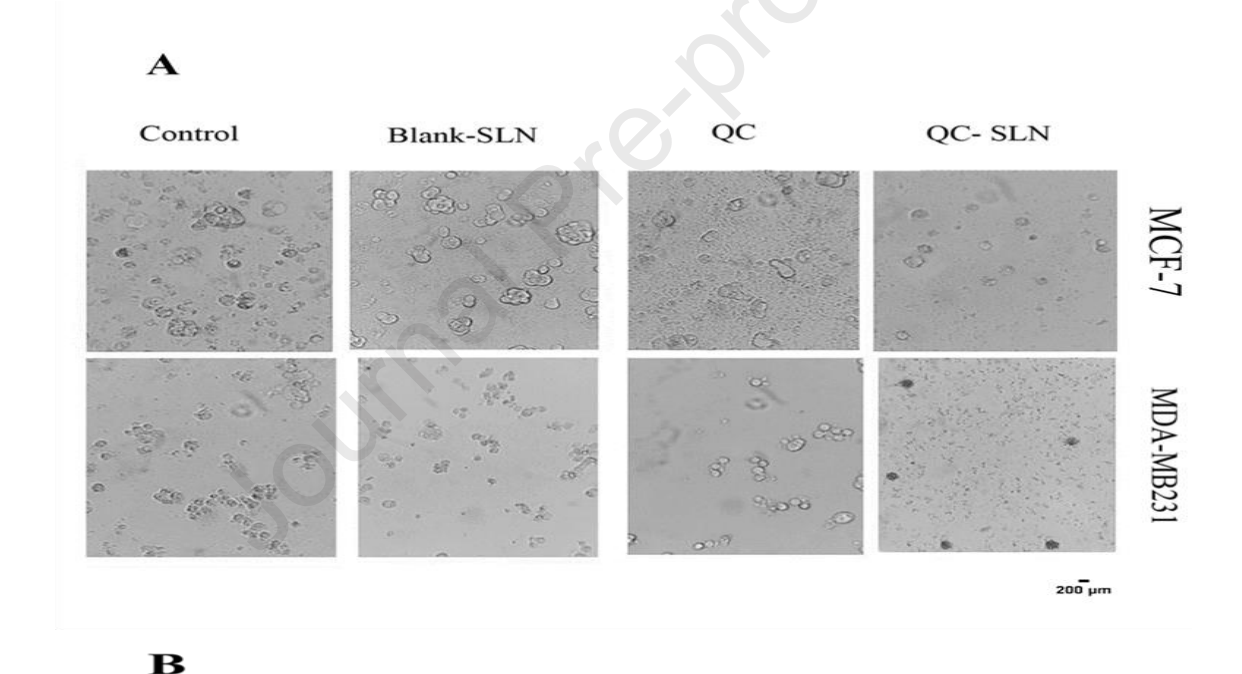
In a previous study, we have previously demonstrated that the treatment with QC-SLN resulted in IC<sub>50</sub> values of 18.9  $\mu$ M, 13.4  $\mu$ M, and >50  $\mu$ M in MCF-7, MDA-MB-231, and MRC5, respectively (Supplementary Figure S4). To compare the effects of QC and QC-SLN, ruled out the impact of Blank-SLN." by using equal concentrations of QC, QC-SLN, and Blank-SLN for the remaining experiments, based on the IC<sub>50</sub> of QC-SLN (Supplementary Figure S5).

### 3.5. Quantitative Real-Time RT-PCR

Supplementary Figure 6 shows that Blank-SLN did not exhibit significant differences in gene expression in either cell line (MCF-7: A and B; MDA-MB231: C and D). In the QC group, MCF-7 cells exhibited a significant increase in E-cad gene expression and a significant decrease in ZEB1 gene expression compared to the control group (Supplementary Figures 6A and 6B), while MDA-MB231 cells showed a significant decrease in ZEB1, VIM, and CD44 gene expression (Supplementary Figures 6C and 6D). In QC-SLN, both MCF-7 and MDA-MB231 cells exhibited a significant reduction in gene expression of ZEB1, VIM, CD44, and N-cad, as well as a significant increase in E-cad gene expression compared to the QC group. QC significantly reduced β-catenin gene expression in MCF-7 cells, but not in MDA-MB231 cells. However, in both cell lines, QC-SLN resulted in a significant decrease in β-catenin gene expression compared to QC (Supplementary Figure 6E).

# 3.6. Spheroid Formation Analysis

To assess the effects of QC and QC-SLN on the characteristics of cancer stem cells (CSCs) in MCF7 and MDA-MB231 cell lines, we conducted a sphere-forming assay. Specifically, cells were incubated in low- attachment plates with a CSC medium for seven days to allow for the formation of sphere structures consisting of CSCs. Following this, cells were treated with 18.9 and 13.4 µM of QC-SLN and QC, respectively. As illustrated in Figure 2, no significant difference in sphere formation was observed between the Blank-SLN group and the control group in either cell line. While the number of spheres decreased in the QC group of both MCF7 and MDA-MBA cells, this change was not statistically significant. Conversely, a significant decrease in the number of spheres was observed in the QC-SLN group compared to both the control and QC groups. This reduction in sphere formation was consistent across both cell lines, albeit slightly more pronounced in MDA-MB-231 than in MCF-7.



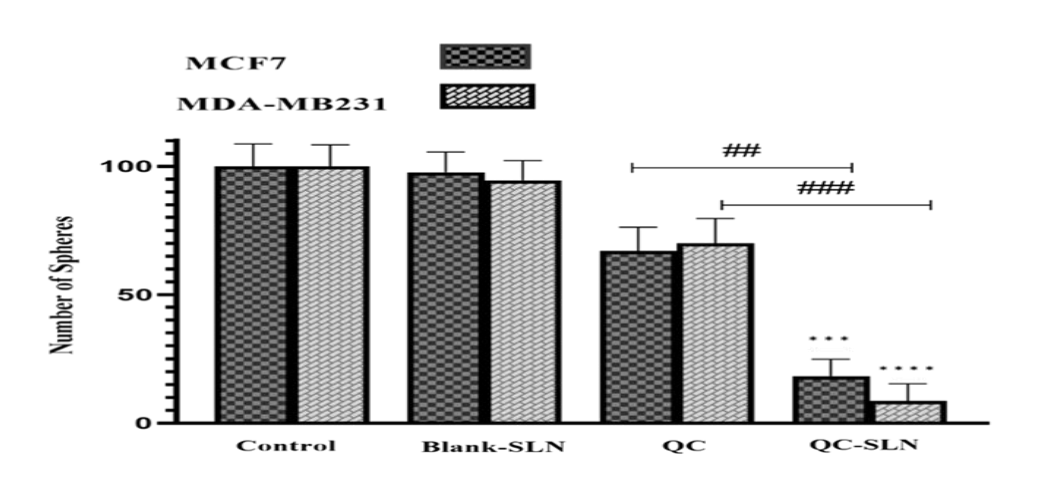


Figure 2. the sphere-forming assay of MCF-7 and MDA-MB231. The photograph sphere-forming of both cell lines in the untreated and treated groups with blank SLN, QC, and QC-SLN for 48 h (A). quantitative illustration of the number in MCF-7 and MDA-MB231 showed in part B, as mean  $\pm$ SD. number of spheres counted using ImageJ. \*\*\*P < 0.001, \*\*\*\*P < 0.001 compared with control group, ## P < 0.01, ###P < 0.001 compared with QC group.

# 3.7. Cell migration Analysis

We evaluated the effects of QC and QC-SLN on tumor cell migration using a wound-healing assay (Figure 3A, B). Breast cancer cells were treated with QC or QC-SLN for 24 or 48 hours. Our results showed a significant decrease in the rate of wound closure in both cell lines after 24 hours of QC treatment, but not after 48 hours (Figure 3C, D). On the other hand, treatment with QC-SLN significantly reduced the rate of wound closure in both cell lines at both 24 and 48 hours, as indicated by the migration indices.

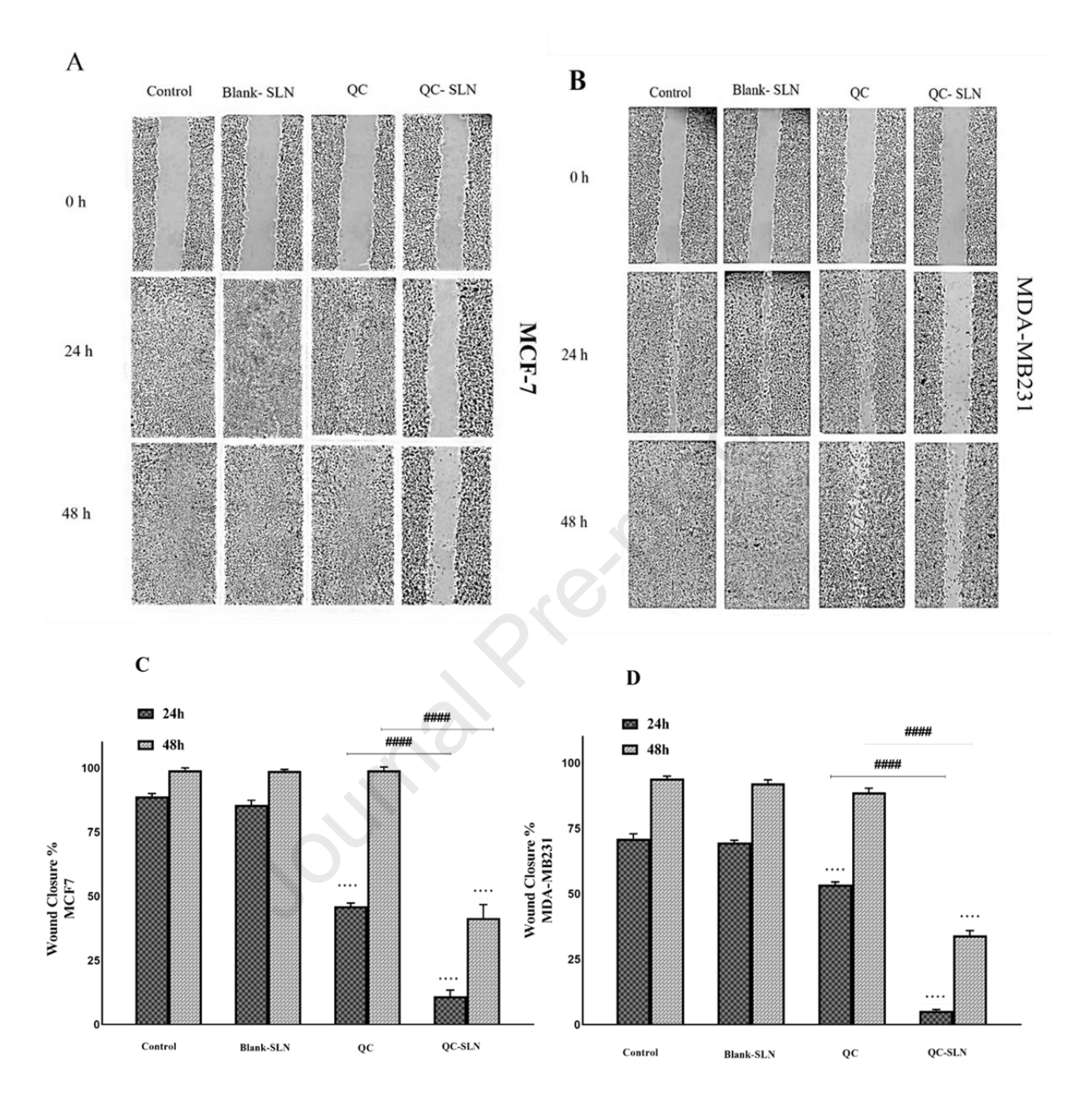


Figure 3. MCF7 and MDA-MB-231 cell migration after 24 and 48 hours of treatment with QC-SLN and QC. The photograph of wound-healing of both cell lines in the untreated and treated groups with blank SLN, QC, and QC-SLN for 24 and 48 h (A and B). wound area measured using ImageJ and quantification values were shown as mean  $\pm$ SD (C, D). \*\*\*\*P < 0.0001; compared with control group, #### P < 0.0001 compared with QC group.

# 3.8. Western Analysis

As illustrated in Figure 4, the impact of blank-SLN on the protein expression of  $\beta$ -catenin, p-Smad-2, and p-Smad-3 in both breast cancer cell lines was negligible. However, treatment with QC significantly reduced  $\beta$ -catenin expression in both cell lines (Figure 4C). Only MCF-7 exhibited a significant reduction in p-Smad-2 expression in response to QC treatment, while no significant changes were observed in MDA-MB231 (Figure 4D). QC treatment did not significantly alter the expression of p-Smad-3 in either cell line (Figure 4E). In contrast, QC-SLN treatment led to a more pronounced decrease in the expression of  $\beta$ -catenin, p-Smad-2, and p-Smad-3 than QC treatment in both MDA-MB231 and MCF-7 cell lines (Figure 4C, D, and E).

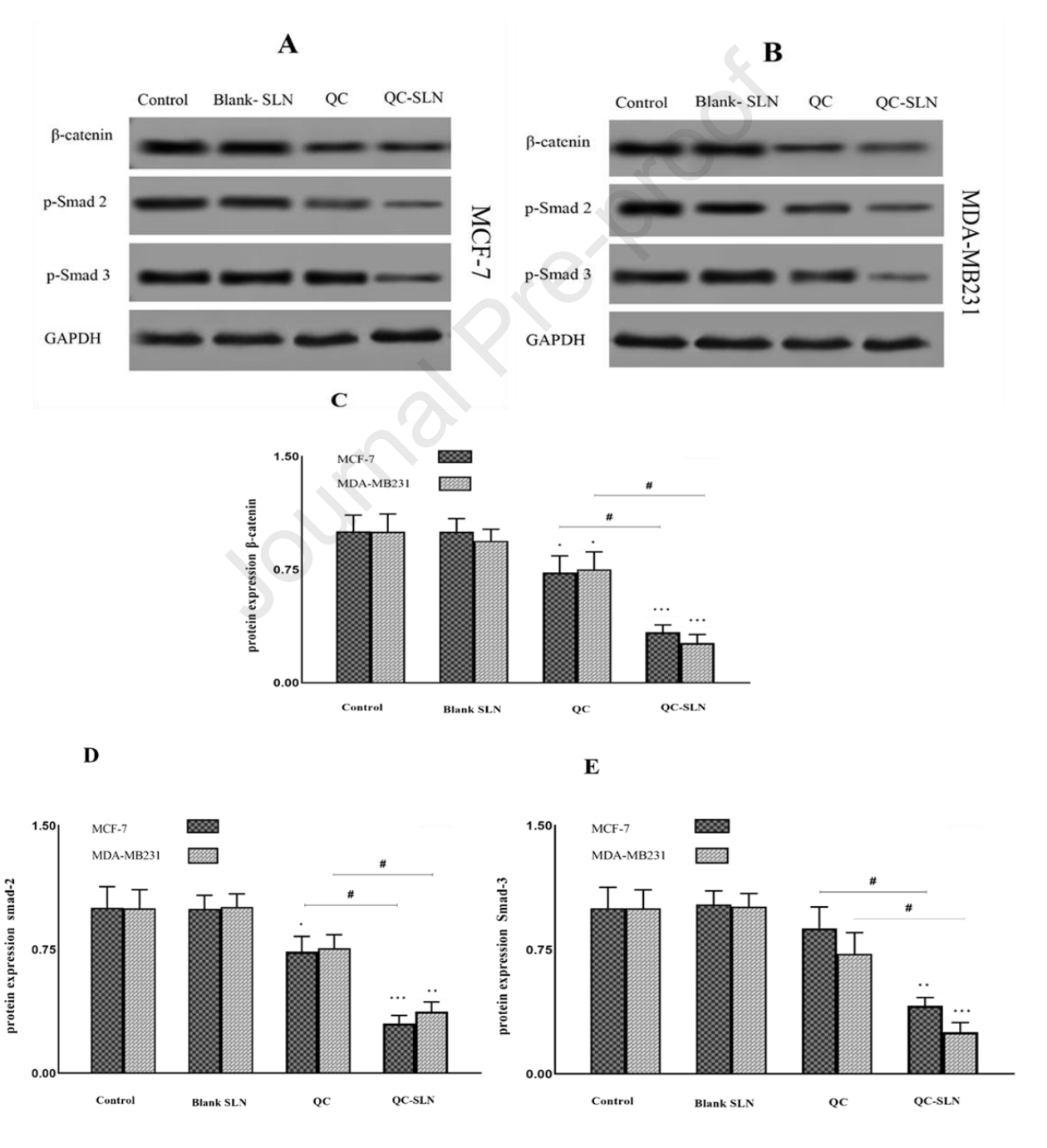


Figure 4. Protein expression of  $\beta$ -catenin, p-Smad-2, and p-Smad-3 in MCF-7 and MDA-MB231. protein bands of  $\beta$ -catenin and p-Smad-2 and 3 in the control and treatment groups in MCF-7 (A) and MDA-MB231(B). Quantification of protein expression of  $\beta$ -catenin(C), p-Smad-2 (D), and p-Smad-3(E) in MCF-7 and MDA-MB231.data was shown as the mean  $\pm$ SD.\* P < 0.05, \*\*\* P < 0.01, and \*\*\*\* P < 0.001 compared to the control group. # P < 0.05, compared to the QC group.

#### Discuusion

Two important barriers to cancer therapy are the resistance of the cancer cells to therapy and recurrence, which are the properties of CSCs. So by overcoming the generation and viability of CSCs, the cancer therapy will be optimized. Chemotherapy, as one of the most important strategies in cancer treatment, is associated with a variety of side effects, so researchers are now focusing on natural remedies. One of these natural components is QC, which, according to previous studies, has inhibitory effects on CSCs [4,31]. A critical problem of QC that limits its clinical application and effectiveness is its low bioavailability. The current study demonstrated that using QC-SLN improves bioavailability and, as a result, the inhibitory effect of QC on EMT, the processes involved in CSC generation, and CSC viability.

The EMT process is recognized for its ability to facilitate the generation of CSCs from epithelial cells and is regulated by two critical signaling pathways: Wnt/ $\beta$ -catenin and TGF $\beta$ /Smad 2,3. Two key transcription factors,  $\beta$ -catenin and p-Smad 2,3 play a significant role in promoting the transcription factors associated with the EMT process, such as ZEB1, and CSC markers such as E-cadherin, vimentin, and CD<sub>44</sub> [32].

Previous studies have reported that QC treatment can reduce the expression of the  $\beta$ -catenin gene and protein, as well as the phosphorylation of Smad 2,3. In this current study, we aimed to investigate the effects of QC in both nanoformulations, specifically QC-SLN. Our findings demonstrated that QC treatment resulted in a reduction of p-Smad 2,3 in both MCF-7 and MDA-MB231 breast cancer cell lines, which is consistent with previous research [33,34]. Importantly, we observed that the inhibitory effects of QC-SLN were significantly greater than those of QC alone, indicating that QC-SLN is a more potent inhibitor of EMT regulators than QC.

The assessment of gene expression of ZEB1, E-cad, N-cad, and CD44 as indices of EMT and CSCs provided further evidence supporting our findings. Specifically, treatment with QC resulted in decreased expression of ZEB1, N-cad, and CD44 genes and increased expression of the E-cad gene, likely due to the reduction in β-catenin expression and phosphorylation of Smad 2,3, which is consistent with previous studies [31,32]. Notably, all of these changes in gene expression were observed in response to treatment with QC-SLN and were more pronounced and potent than those observed with QC alone, underscoring the role of QC-SLN in inhibiting the generation of CSCs.

The sphere formation assay was then performed to assess the effect of the changes in protein and gene expression induced by QC and QC-SLN treatments. The assay demonstrated that QC treatment reduced the number of sphere structures composed of CSCs, which is consistent with the findings of previous studies by Xiuli Li et al. and Kashyap A. et al., who reported the inhibitory effect of QC on the proliferation of breast cancer stem cells and downregulation of CD44 gene

expression in the stem cell population [4,31]. The reduction in sphere structures was more significant with QC-SLN treatment than with QC treatment, further indicating the potent effect of QC-SLN in inhibiting the generation and viability of CSCs.

To assess the impact of QC on cell migration, we conducted a wound-healing assay, which is a critical characteristic of CSCs. Our results showed that QC treatment effectively impeded wound closure, a marker of cell migration, especially at 24 hours in both MCF-7 and MDA-MB231 cells. These findings are in line with a recent study by Roshanazadeh et al. (2021), which demonstrated that QC can suppress the migration of MDA-MB-231 breast cancer cells [35-37]. Importantly, QC-SLN treatment significantly and potently hindered the migration of both cell lines, particularly at 24 and 48 hours, compared to QC treatment, indicating the superior potency of QC-SLN in inhibiting migration.

#### Conclusion

This study highlights the potential of QC-SLN as a therapeutic agent for breast cancer stem cells. The results suggest that QC-SLN is a more potent inhibitor of EMT regulators and CSC generation than QC alone, likely due to its improved bioavailability. These findings suggest that natural remedies like QC may offer a promising avenue for cancer therapy. Further in vivo studies are needed to assess the safety and efficacy of QC-SLN in breast cancer treatment. Overall, this study contributes to a growing body of research on natural compounds as potential cancer therapies and underscores the importance of exploring new and innovative approaches to cancer treatment.

# Acknowledgements

The research was financially supported by grant number **CMRC - 9914** from the Cellular and molecular research center, medical basic sciences research institute Ahvaz Jundishapur University of Medical Sciences, Ahvaz, Iran. This paper was extracted from PhD thesis of Mahdi Hatami.

#### **Author contributions**

Dr. Mojtaba Rashidi significantly contributed to the conceptualization and design of the work. Dr. Maryam Kouchak and Layasadat Khorsandi prepared and updated the material. Dr. Alireza Khairullah: data analysis and interpretation. Mahdi Hatami: the acquisition, interpretation, and analysis of data.

**Funding**: The research was financially supported by the Cellular and Molecular Research Center of Ahvaz Jundishapur University of Medical Sciences, Ahvaz, Iran.

#### **Declarations**

**Conflicts of Interest:** We have no conflict of interest to declare.

Ethical approval: IR.AJUMS.REC.1399.509.

**Research involving human and/or animal participants**: This article does not contain any studies with human participants or animals performed by any of the authors.

**Informed consent** All of the authors declare consent to participate and consent for the publication.

# Reference

- [1] R.A. Dar, M. Rasool, A.J.C.i.B. Assad, Medicine, Breast cancer detection using deep learning: Datasets, methods, and challenges ahead, Comput Biol Med. (2022) 106073. https://doi.org/10.1016/j.compbiomed.2022.106073.
- [2] R. Ismail-Khan, M.M.J.C.c. Bui, A review of triple-negative breast cancer, Cancer Control. 17 (2010) 173-176. https://doi.org/10.1177/107327481001700305
- [3] M. Nedeljković, A.J.C. Damjanović, Mechanisms of chemotherapy resistance in triple-negative breast cancer—how we can rise to the challenge, Cells. 8 (2019) 957. https://doi.org/10.3390/cells8090957.
- [4] X. Li, N. Zhou, J. Wang, Z. Liu, X. Wang, Q. Zhang, Q. Liu, L. Gao, R.J.L.s. Wang, Quercetin suppresses breast cancer stem cells (CD44+/CD24-) by inhibiting the PI3K/Akt/mTOR-signaling pathway, Life Sci. 196 (2018) 56-62. https://doi.org/10.1016/j.lfs.2018.01.014.
- [5] J. Bajaj, E. Diaz, T.J.J.o.C.B. Reya, Stem cells in cancer initiation and progression, J CELL BIOL. 219 (2020). https://doi.org/10.1083/jcb.201911053.
- [6] R. Chiotaki, H. Polioudaki, P.J.C.C.D.T. A Theodoropoulos, Cancer stem cells in solid and liquid tissues of breast cancer patients: characterization and therapeutic perspectives, Curr Cancer Drug Targets. 15 (2015) 256-269. https://doi.org/10.2174/1568009615666150211102503.
- [7] Y. Wang, Y.J.E.c.r. Shang, Epigenetic control of epithelial-to-mesenchymal transition and cancer metastasis, Exp Cell Res. 319 (2013) 160-169. https://doi.org/10.1016/j.yexcr.2012.07.019.
- [8] Q. Hu, S. Tong, X. Zhao, W. Ding, Y. Gou, K. Xu, C. Sun, G.J.C.p. Xia, biochemistry, Periostin mediates TGF-β-induced epithelial mesenchymal transition in prostate cancer cells, Cell Physiol Biochem. 36 (2015) 799-809. https://doi.org/10.1159/000430139.
- [9] W. Guo, Z. Keckesova, J.L. Donaher, T. Shibue, V. Tischler, F. Reinhardt, S. Itzkovitz, A. Noske, U. Zürrer-Härdi, G.J.C. Bell, Slug and Sox9 cooperatively determine the mammary stem cell state, Cell. 148 (2012) 1015-1028. https://doi.org/10.1016/j.cell.2012.02.008.
- [10] M.A. Eckert, T.M. Lwin, A.T. Chang, J. Kim, E. Danis, L. Ohno-Machado, J.J.C.c. Yang, Twist1-induced invadopodia formation promotes tumor metastasis, Cancer Cell. 19 (2011) 372-386. https://doi.org/10.1016/j.ccr.2011.01.036.
- [11] A. Martínez-Ramírez, M. Díaz-Muñoz, A. Butanda-Ochoa, F.J.P.s. Vázquez-Cuevas, Nucleotides and nucleoside signaling in the regulation of the epithelium to mesenchymal transition (EMT), Purinergic Signal. 13 (2017) 1-12. https://doi.org/10.1007/s11302-016-9550-3
- [12] S.-G. Pohl, N. Brook, M. Agostino, F. Arfuso, A.P. Kumar, A.J.O. Dharmarajan, Wnt signaling in triplenegative breast cancer, Oncogenesis. 6 (2017) e310-e310. https://doi.org/10.1038/oncsis.2017.14
- [13] S. Srivastava, R.R. Somasagara, M. Hegde, M. Nishana, S.K. Tadi, M. Srivastava, B. Choudhary, S.C.J.S.r. Raghavan, Quercetin, a natural flavonoid interacts with DNA, arrests cell cycle and causes tumor regression by activating mitochondrial pathway of apoptosis, Sci Rep. 6 (2016) 1-13. http://dx.doi.org/10.1038/srep24049.
- [14] R. Tummala, W. Lou, A.C. Gao, N.J.M.c.t. Nadiminty, Quercetin Targets hnRNPA1 to Overcome Enzalutamide Resistance in Prostate Cancer CellsQuercetin Targets hnRNPA1 and Synergizes with Enzalutamide, Mol Cancer Ther. 16 (2017) 2770-2779. https://doi.org/10.1158/1535-7163.MCT-17-0030.
- [15] D.W. Lamson, M.S.J.A.m.r.a.j.o.c.t. Brignall, Antioxidants and cancer, part 3: quercetin, A J Clin Med Ther. 5 (2000) 196-208.
- [16] J.M. Davis, E.A. Murphy, M.D.J.C.s.m.r. Carmichael, Effects of the dietary flavonoid quercetin upon performance and health, Curr Sports Med Rep. 8 (2009) 206-213. https://10.1249/JSR.0b013e3181ae8959.

- [17] S.S. Dhumale, B.N. Waghela, C.J.I.I. Pathak, Quercetin protects necrotic insult and promotes apoptosis by attenuating the expression of RAGE and its ligand HMGB1 in human breast adenocarcinoma cells, IUBMB Life. 67 (2015) 361-373. https://doi.org/10.1002/iub.1379.
- [18] A. Rauf, M. Imran, I.A. Khan, M. ur-Rehman, S.A. Gilani, Z. Mehmood, M.S.J.P.R. Mubarak, Anticancer potential of quercetin: A comprehensive review, Phytother Res. 32 (2018) 2109-2130. https://doi.org/10.1002/ptr.6155.
- [19] A.A. Abd-Rabou, H.H.J.A.i.m.s. Ahmed, CS-PEG decorated PLGA nano-prototype for delivery of bioactive compounds: A novel approach for induction of apoptosis in HepG2 cell line, Adv Med Sci. 62 (2017) 357-367. https://doi.org/10.1016/j.advms.2017.01.003.
- [20] B. Stella, E. Peira, C. Dianzani, M. Gallarate, L. Battaglia, C.L. Gigliotti, E. Boggio, U. Dianzani, F.J.N. Dosio, Development and characterization of solid lipid nanoparticles loaded with a highly active doxorubicin derivative, Nanomaterials. 8 (2018) 110. https://doi.org/10.3390/nano8020110.
- [21] W. Wang, T. Chen, H. Xu, B. Ren, X. Cheng, R. Qi, H. Liu, Y. Wang, L. Yan, S.J.M. Chen, Curcumin-loaded solid lipid nanoparticles enhanced anticancer efficiency in breast cancer, Molecules. 23 (2018) 1578. https://doi.org/10.3390/molecules23071578.
- [22] R. Abbasalipourkabir, A. Salehzadeh, R.J.J.o.e.n. Abdullah, Tamoxifen-loaded solid lipid nanoparticles-induced apoptosis in breast cancer cell lines, J Exp Nanosci. 11 (2016) 161-174. https://doi.org/10.1080/17458080.2015.1038660.
- [23] N.M. Badawi, M.H. Teaima, K.M. El-Say, D.A. Attia, M.A. El-Nabarawi, M.M.J.I.j.o.n. Elmazar, Pomegranate extract-loaded solid lipid nanoparticles: design, optimization, and in vitro cytotoxicity study, Int J Nanomedicine. 13 (2018) 1313. https://doi: 10.2147/IJN.S154033.
- [24] J. Sun, C. Bi, H.M. Chan, S. Sun, Q. Zhang, Y.J.C. Zheng, s.b. biointerfaces, Curcumin-loaded solid lipid nanoparticles have prolonged in vitro antitumour activity, cellular uptake and improved in vivo bioavailability, Colloids Surf B Biointerfaces. 111 (2013) 367-375. https://doi.org/10.1016/j.colsurfb.2013.06.032.
- [25] A. Vijayakumar, R. Baskaran, Y.S. Jang, S.H. Oh, B.K.J.A.P. Yoo, Quercetin-loaded solid lipid nanoparticle dispersion with improved physicochemical properties and cellular uptake, AAPS PharmSciTech. 18 (2017) 875-883. http://dx.doi.org/10.1208/s12249-016-0573-4.
- [26] R. Abbasalipurkabir, A. Salehzadeh, R.J.P.T. Abdullah, Delivering tamoxifen within solid lipid nanoparticles, Pharm Technol. 35 (2011) 74-79.
- [27] S. Nie, W.L. Hsiao, W. Pan, Z. Yang, Thermoreversible Pluronic F127-based hydrogel containing liposomes for the controlled delivery of paclitaxel: in vitro drug release, cell cytotoxicity, and uptake studies, Int J Nanomedicine. 6 (2011) 151-166. http://10.2147/ijn.S15057
- [28] U.-H. Park, J.-C. Jeong, J.-S. Jang, M.-R. Sung, H. Youn, S.-J. Lee, E.-J. Kim, S.-J.J.B. Um, P. Bulletin, Negative regulation of adipogenesis by kaempferol, a component of Rhizoma Polygonati falcatum in 3T3-L1 cells, Biol Pharm Bull. 35 (2012) 1525-1533. https://doi.org/10.1248/bpb.b12-00254.
- [29] K. Munakata, M. Uemura, I. Takemasa, M. Ozaki, M. Konno, J. Nishimura, T. Hata, T. Mizushima, N. Haraguchi, S.J.I.j.o.o. Noura, SCGB2A1 is a novel prognostic marker for colorectal cancer associated with chemoresistance and radioresistance, Int J Onco. 44 (2014) 1521-1528. https://doi.org/10.3892/ijo.2014.2316.
- [30] F. Niazvand, M. Orazizadeh, L. Khorsandi, M. Abbaspour, E. Mansouri, A.J.M. Khodadadi, Effects of quercetin-loaded nanoparticles on MCF-7 human breast cancer cells, Medicina. 55 (2019) 114. https://doi.org/10.3390/medicina55040114.
- [31] A. Kashyap, S.M. Umar, M. Mendiratta, C.P.J.P.P. Prasad, In vitro anticancer efficacy of a polyphenolic combination of Quercetin, Curcumin, and Berberine in triple negative breast cancer (TNBC) cells, Phytomed Plus. 2 (2022) 100265. https://doi.org/10.1016/j.phyplu.2022.100265.
- [32] Y.-C. Hseu, Y.-C. Lin, P. Rajendran, V. Thigarajan, D.C. Mathew, K.-Y. Lin, T.-D. Way, J.-W. Liao, H.-L.J.F. Yang, C. Toxicology, Antrodia salmonea suppresses invasion and metastasis in triple-negative

#### Journal Pre-proof

- breast cancer cells by reversing EMT through the NF- $\kappa$ B and Wnt/ $\beta$ -catenin signaling pathway, Food Chem Toxicol. 124 (2019) 219-230. https://doi.org/10.1016/j.fct.2018.12.009.
- [33] Y. Guo, Y. Tong, H. Zhu, Y. Xiao, H. Guo, L. Shang, W. Zheng, S. Ma, X. Liu, Y.J.C.B. Bai, Toxicology, Quercetin suppresses pancreatic ductal adenocarcinoma progression via inhibition of SHH and TGF-β/Smad signaling pathways, Cell Biol Toxicol. 37 (2021) 479-496. https://doi.org/10.1007/s10565-020-09562-0
- [34] J. Feng, D. Song, S. Jiang, X. Yang, T. Ding, H. Zhang, J. Luo, J. Liao, Q.J.B. Yin, b.r. communications, Quercetin restrains TGF- $\beta$ 1-induced epithelial—mesenchymal transition by inhibiting Twist1 and regulating E-cadherin expression, Biochem Biophys Res Commun. 498 (2018) 132-138. https://doi.org/10.1016/j.bbrc.2018.02.044
- [35] S.R. Kim, E.Y. Lee, D.J. Kim, H.J. Kim, H.R.J.M. Park, Quercetin inhibits cell survival and metastatic ability via the EMT-mediated pathway in oral squamous cell carcinoma, Molecules. 25 (2020) 757. https://doi.org/10.3390/molecules25030757
- [36] N.-T. Trinh, T.M.N. Nguyen, J.-I. Yook, S.-G. Ahn, S.-A.J.P. Kim, Quercetin and Quercitrin from Agrimonia pilosa Ledeb Inhibit the Migration and Invasion of Colon Cancer Cells through the JNK Signaling Pathway, Pharmaceuticals. 15 (2022) 364. https://doi.org/10.3390/ph15030364 [37] M. Roshanazadeh, H.B. Rezaei, M.J.I.J.o.B.M.S. Rashidi, Quercetin synergistically potentiates the anti-metastatic effect of 5-fluorouracil on the MDA-MB-231 breast cancer cell line, Iran J Basic Med Sci. 24 (2021) 928. https://doi.org/10.5812/ijcm.119049

# **Highlights**

QC-SLNs significantly reduced cell viability, migration, and sphere formation in MDA-MB231 cells.

QC-SLNs reduced the protein expression of  $\beta$ -catenin and p-Smad 2 and 3, and gene expression of CD<sub>44</sub>, zinc finger E-box binding homeobox 1 (ZEB1), and vimentin, while increasing the gene expression of E-cadherin.

SLNs improved the cytotoxic effect of QC in MDA-MB231 cells by increasing its bioavailability and inhibiting epithelial-mesenchymal transition (EMT), thereby effectively inhibiting CSC generation.

SLNs could be a promising new treatment for triple-negative breast cancer (TNBC), but more in vivo studies are needed to confirm their efficacy.

# **Conflict of Interest**

Effective Inhibition of Breast Cancer Stem Cell Properties by Quercetin-Loaded Solid Lipid Nanoparticles via Reduction of Smad2/Smad3 Phosphorylation and  $\beta$ -Catenin Signaling Pathway in Triple-Negative Breast Cancer

Mahdi Hatami<sup>1,2</sup>, Maryam Kouchak<sup>3,4</sup>, Alireza Kheirollah<sup>2</sup>, Layasadat Khorsandi<sup>1</sup>, Mojtaba Rashidi<sup>1,2\*</sup>

<sup>1</sup>Cellular and Molecular Research Center, Medical Basic Sciences Research Institution, Ahvaz Jundishapur University of Medical Sciences, Ahvaz, Iran.

#### Conflict of Interest

The authors declares that they have no conflict of interest regarding the content of this article.

<sup>&</sup>lt;sup>2</sup> Department of Clinical Biochemistry, Faculty of Medicine, Ahvaz Jundishapur University of Medical Sciences, Ahvaz, Iran

<sup>&</sup>lt;sup>3</sup> Nanotechnology Research Center, Ahvaz Jundishapur University of Medical Sciences, Ahvaz, Iran

<sup>&</sup>lt;sup>4</sup> Department of Pharmaceutics, Faculty of Pharmacy, Ahvaz Jundishapur University of Medical Sciences, Ahvaz, Iran